04,09

Luminescent properties of solid solutions of yttrium-scandium phosphates doped with europium ions

© V.S. Voznyak-Levushkina[1], A.A. Arapova[1], D.A. Spassky[2,3], I.V. Nikiforov[4], B.I. Zadneprovsky[5]

[1] Faculty of Physics, Lomonosov Moscow State University,
Moscow, Russia
[2] Skobeltsyn Institute of Nuclear Physics, Moscow State University,
Lomonosov Moscow State University,
Moscow, Russia
[3] Institute of Physics, University of Tartu,
50411 Tartu, Estonia
[4] Department of Chemistry, Moscow State University,
Moscow, Russia
[5] All-Russian Scientific Research Institute of Mineral Resources,
Aleksandrov, Russia

E-mail: levushkina@physics.msu.ru

Received July 25, 2022
Revised July 25, 2022
Accepted July 26, 2022

The luminescent properties of solid solutions $Y_{1-x}Sc_xPO_4$: 0.5 mol.% Eu^{3+} ($x = 0, 0.2, 0.4, 0.5, 0.6, 0.8, 1$) under excitation by ultraviolet and vacuum-ultraviolet radiation were studied. The influence of disorder of the crystal structure in solid solutions on the structure of Eu^{3+} luminescence spectra is shown. A non-linear dependence of values of the optical band gap on solid solution composition was obtained and a model was suggested to explain this effect.

Keywords: energy transfer, luminescence, solid solutions, $ScPO_4:Eu^{3+}$, $YPO_4:Eu^{3+}$.

DOI: 10.21883/PSS.2022.12.54383.449

1. Introduction

Lanthanoid-doped orthophosphates are being widely studied due to their possible application in various fields of science and engineering. In particular, orthophosphates are suggested for plasma panels [1], scintillation detectors [2], light-emitting diode [3], solar panels [4], thermal barrier coatings [5] and optical thermometry [6]. Among the many orthophosphates of rare earth elements, phosphors based on YPO_4 and $ScPO_4$ attract particular attention due to their high thermal, chemical and radiation stability, as well as excellent luminescent properties [3,7]. The wide area of potential application of these phosphates explains the interest in their further study and improvement of luminescent properties. The formation of orthophosphate-based solid solutions is a possible way to solve this task.

The structure of luminescence spectra of Eu^{3+} ions, conditioned by intraconfiguration $^5D_0 \rightarrow {}^7F_J$ transitions, is sensitive to environment symmetry, so that the given ion can be used as a luminescent probe. It has been demonstrated earlier that a disorder of the crystal structure in solid solutions of phosphates due to a statistical distribution of substitution cations across the lattice sites, causes widening and shift of Eu^{3+} luminescence bands [8] and makes it possible to obtain additional information about the peculiarities of symmetry of luminescence centers. A gradual change of solid solution composition allows for adjusting its luminescent properties and making a compound with the specified characteristics. For instance, it was shown for solid solutions $Lu_3(Al_xGa_{1-x})_5O_{12}$ that gradual substitution of Al^{3+} by Ga^{3+} ions leads to a decrease of the band gap and an overlap of energy levels of defects with electronic states of the conduction band bottom, thus reducing the adverse influence of shallow traps on energy transfer and improving the kinetic characteristics of Ce^{3+} luminescence [9,10].

Another interesting effect found in solid solutions is a non-linear increase of luminescence intensity for intermediate concentrations of substitution cations [11–14]. For instance, solid solution $Gd_{0.5}Y_{0.5}PO_4:Tb^{3+}$ was characterized by a twofold increase of luminescence intensity as compared to $YPO_4:Tb^{3+}$ [15]. The effect was attributed to peculiarities of morphology and phase composition of the studied solid solution. However, intensity does not always increase. Solid solutions $Lu_xY_{1-x}PO_4$:Eu features a gradual decrease of luminescence intensity with an increase of x [8]. The obtained dependence was explained by a higher mobility of low-energy electrons in the conduction band with an increase of lutetium content in solutions.

The influence of composition on luminescence intensity of solid solutions $Y_{1-x}Sc_xPO_4:Eu^{3+}$ has been previously studied in [16]. The solid solutions featured an increase of luminescence intensity with the maximum at $x = 0.5$, which was associated with an increased efficiency of energy transfer from the matrix to luminescence centers and

a decrease of nonradiative energy losses. Thereat, the luminescence spectra of $YPO_4:Eu^{3+}$ revealed additional bands not typical for Eu^{3+} luminescence in the given matrix, which indicated the presence of impurity phases in the studied samples and was related to a low temperature of solution synthesis.

In the present paper we study the influence of composition of solid phosphate solutions $Y_{1-x}Sc_xPO_4:Eu^{3+}$ ($x = 0$, 0.2, 0.4, 0.5, 0.6, 0.8, 1) on the structure of activator's luminescence spectra. The luminescence excitation spectra are analyzed to show the peculiarities of formation of electronic states of the conduction band bottom and upper edge of the valence band and their influence on a change of optical band gap with a change in solution composition.

2. Experimental procedure

The samples of solid phosphate solutions $Y_{1-x}Sc_xPO_4:0.5$ mol.% Eu^{3+}, where $x = 0$, 0.2, 0.4, 0.5, 0.6, 0.8, 1 were synthesized by the sol-gel method. Synthesis consisting of several stages, including solubilization of non-water-soluble oxides, preparation of reaction mixture containing ions of rare earth elements and the dissolved form of boric acid, followed by deposition of the obtained product. The material obtained by synthesis was crystallized at the last stage. To do so, the sample underwent high-temperature annealing under the following conditions: annealing temperature 960°C, holding time 2 h, atmosphere — air. A study of the synthesized phosphates by the X-ray diffraction method did not reveal additional phases in the solid solutions, but additional bands were found in the luminescence spectra of YPO_4 [16]. This indicates that the luminescent method is more sensitive to revelation of additional phases as compared to the X-ray diffraction analysis method. The problem of the presence of an additional phase was solved by additional annealing of the whole series at 1450°C for 20 h. According to [17], this temperature is sufficient for formation of the whole series of solid solutions $Y_{1-x}Sc_xPO_4$. After annealing, the structure of the $YPO_4:Eu^{3+}$ luminescence spectrum corresponded to the structure given in the literature [18].

The luminescence spectra and spectra of luminescence excitation in the ultraviolet (UV) and vacuum-ultraviolet (VUV) ranges were measured using specialized units for luminescence spectroscopy of solid bodies. The excitation source for spectroscopy in the UV-range was a 150 W xenon lamp, excitation wavelength was chosen using a MDR-206 primary monochromator. The samples were placed in a Cryotrade LN-120 vacuum optical cryostat. Luminescence was recorded using an Oriel MS257 spectrograph equipped with a Marconi 30-11 CCD detector having the spectral resolution of 0.3 nm. The luminescence spectra were corrected for the instrument function.

Measurements in the UV-VUV spectrum region (130–400 nm) were performed using a Hamamatsu L11798 deuterium lamp with a window of MgF_2 as the excitation source. Monochromatization of the lamp radiation was performed using a McPherson 234/302 vacuum primary monochromator. The samples were placed in an ARS vacuum cryostat that allows for measurements in the temperature range of 5–300 K. The luminescence spectrum was recorded using a Shamrock 303i monochromator equipped with a Hamamatsu H8259 counting head. All measurements were performed at 300 K.

3. Results and discussion

3.1. Luminescence spectra $Y_{1-x}Sc_xPO_4:Eu^{3+}$

The luminescence spectra for the series of solid solutions $Y_{1-x}Sc_xPO_4:Eu^{3+}$ are shown in Fig. 1. The most intensive narrow luminescence bands in the region of 580–720 nm are related to intraconfiguration $^5D_0-^7F_{0-4}$ transitions in the $4f$-shell of Eu^{3+} ions. The structure of the luminescence bands depends on symmetry of the europium ion environment. It is known that yttrium and scandium phosphates pertain to the structure type of xenotime, which is isostructural to zirconium ($ZrSiO_4$),and have a tetragonal crystal system with space group $I4_1/amd$, $Z = 4$ [19–21]. The crystal lattice sites where Sc or Y is located are characterized by symmetry group D_{2d}. Each cation is surrounded by eight O^{2-} ions and has two different lengths of the cation to oxygen bond, thus forming a distorted dodecahedron (Fig. 2), while oxyanion groups PO_4 are a distorted tetrahedron. An europium ion substitutes a Y^{3+} or Sc^{3+} cation in the crystal lattice, and Eu chiefly occupies the place of Y, given their closer ionic radii, the coordination number being equal to 8 — Y^{3+} (1.02 Å), Eu^{3+} (1.087 Å), Sc^{3+} (0.87 Å) [22].

The spectral line of an Eu^{3+} ion located at a site with symmetry D_{2d} must have two components corresponding to a magnetic dipole transition $^5D_0-^7F_1$, and 2, 3, 3 for transitions $^5D_0-^7F_2$, $^5D_0-^7F_3$, $^5D_0-^7F_4$ respectively [23]. The peaks obtained herein for $YPO_4:Eu^{3+}$ were identified

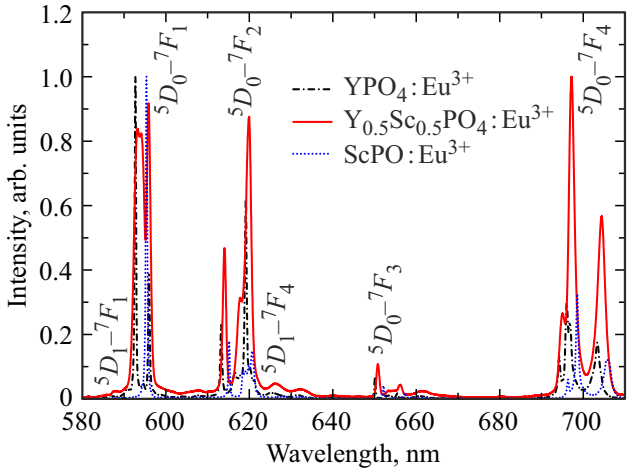

Figure 1. Luminescence spectra of solid solutions $Y_{1-x}Sc_xPO_4:Eu^{3+}$, $\lambda_{ex} = 397$ nm.

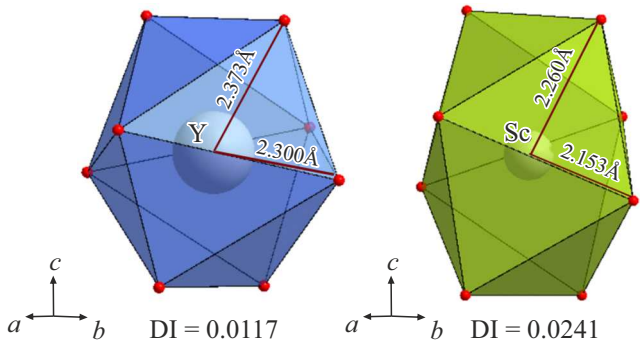

Figure 2. Polyhedra YO_8 and ScO_8 in YPO_4 and $ScPO_4$ structures respectively.

according to paper [18], the results are given in the table. It should be noted that, in addition to transitions from the $^5D_0$ level, the spectrum also contains low-intensity groups of luminescence bands, which correspond to transitions from the higher $^5D_1$ level: $^5D_1-{}^7F_4$ (615–618, 620–633 nm), $^5D_1-{}^7F_3$ (583–588 nm) (Fig. 1). The region of 550–580 nm contains several other low-intensity peaks related to a $^5D_1-{}^7F_2$ transition.

The low intensity of transitions from the $^5D_1$ level is related to the nonradiative process of energy transfer between two Eu^{3+} ions with the participation of phonons as follows: ion 1 being in state $^5D_1$ relaxes to state $^5D_0$, while the liberated energy (with the help of phonons) enables the neighboring ion 2 to go from the ground state $^7F_0$ to state $^7F_{1-4}$ [24].

The recorded luminescence spectra for $ScPO_4:Eu^{3+}$ also agree with the literature data [7]. Europium substitutes Y^{3+} and Sc^{3+} cations and occupies dodecahedral sites with centrosymmetric point group D_{2d}, for which the $^5D_0-{}^7F_0$ transition is prohibited. The luminescence band corresponding to this transition is characterized by a very low intensity in the luminescence spectra of $YPO_4:Eu^{3+}$ and $ScPO_4:Eu^{3+}$ (Fig. 3, *a*). A disorder of the crystal structure in solid solutions causes a decrease of symmetry of crystal lattice sites where Eu^{3+} is located, and partial enabling of the $^5D_0-{}^7F_0$ transition in the 580 nm region, which allows for reliable recording of this band for solid solutions. The highest band intensity was recorded for sample with $x = 0.5$, which indicates the greatest distortions of point symmetry of the site where Eu^{3+} is located. The position of band $^5D_0-{}^7F_0$ shifts to the long-wave region when x increases (Fig. 3, *b*). It is known that position of the band corresponding to the $^5D_0-{}^7F_0$ transition depends on length of the Eu–O bond due to the influence of the nephelauxetic effect [25] and shifts towards greater wavelengths when the Eu–O distance decreases. In $Y_{1-x}Sc_xPO_4:Eu^{3+}$, when a Y^{3+} cation is substituted by Sc^{3+}, the unit cell volume and constants decrease due to a smaller ionic radius of Sc^{3+}. This, in addition to a decrease of the distance between Eu and O, on the whole causes a change in the force of the crystalline field, which determines the position of the Eu^{3+} luminescence bands (Fig. 4, *a*).

Widening of the luminescence bands was also observed in solid solutions $Y_{1-x}Sc_xPO_4:Eu^{3+}$. Fig. 4, *b* shows the dependence of the luminescence band's full width at half maximum (FWHM), which corresponds to the $^5D_0-{}^7F_2$ transition, on value of x in the solid solution. The FWHM value is determined by the multitude of different local symmetries of the Eu^{3+} luminescence center. The average number of substitution cations (Y^{3+} or Sc^{3+}), located in the second coordination sphere, is determined by the value of x, however, their exact quantity varies from cell to cell. The maximum quantity of various combinations of Y^{3+}/Sc^{3+} substitution cations in a unit cell is reached at $x = 0.5$, which causes the greatest disorder of the crystal lattice for the $Y_{0.5}Sc_{0.5}PO_4:Eu^{3+}$ sample, and, consequently, the maximum widening of the luminescence band.

It should be noted that splitting is observed for several luminescence bands in solid solutions, in addition to shifting and widening. Thus, a single narrow band was recorded for $YPO_4:Eu^{3+}$ at 592.70 nm, which corresponds to a transition from the $^5D_0(A_1)$ level to the doubly degenerate $^7F_1(E)$ level. This band in solid solutions splits into two widened lines (Fig. 5). A doublet structure forms because of a decrease of the symmetry of the Eu luminescence center due to a distortion of the crystal lattice in solid solutions and withdrawal of degeneration of the $^7F_1(E)$ level. Thus, the luminescence spectra in solid solutions in the region of the $^5D_0-{}^7F_1$ transition are represented by three bands.

Position of luminescence bands for $YPO_4:Eu^{3+}$ and their interpretation according to paper [18]

Transition	Spectral position of luminescence band, nm
$^5D_0(A_1)-{}^7F_0(A_1)$	581.10
$^5D_1(E)-{}^7F_3(B_2)$	583.80
$^5D_1(A_2)-{}^7F_3(B_1)$	586.76
$^5D_1(E)-{}^7F_3(B_1)$	587.40
$^5D_1(E)-{}^7F_3(E^{(1)})$	588.10
$^5D_0(A_1)-{}^7F_1(E)$	592.70
$^5D_0(A_1)-{}^7F_1(A_2)$	596.00
$^5D_0(A_1)-{}^7F_2(B_2)$	613.27
$^5D_1(E)-{}^7F_4(A_1^{(2)})$	616.53
$^5D_1(A_2)-{}^7F_4(B)$	617.66
$^5D_0(A_1)-{}^7F_2(E)$	619.16
$^5D_1(E)-{}^7F_4(B_2)$	620.25
$^5D_1(A_2)-{}^7F_4(E^{(1)})$	625.30
$^5D_1(E)-{}^7F_4(A_1^{(1)})$	631.40
$^5D_0(A_1)-{}^7F_3(B_2)$	650.10
$^5D_0(A_1)-{}^7F_3(E)$	652.03
$^5D_0(A_1)-{}^7F_3(E)$	655.45
$^5D_0(A_1)-{}^7F_4(E^{(2)})$	694.24
$^5D_0(A_1)-{}^7F_4(B_2)$	696.00
$^5D_0(A_1)-{}^7F_4(E^{(1)})$	703.37

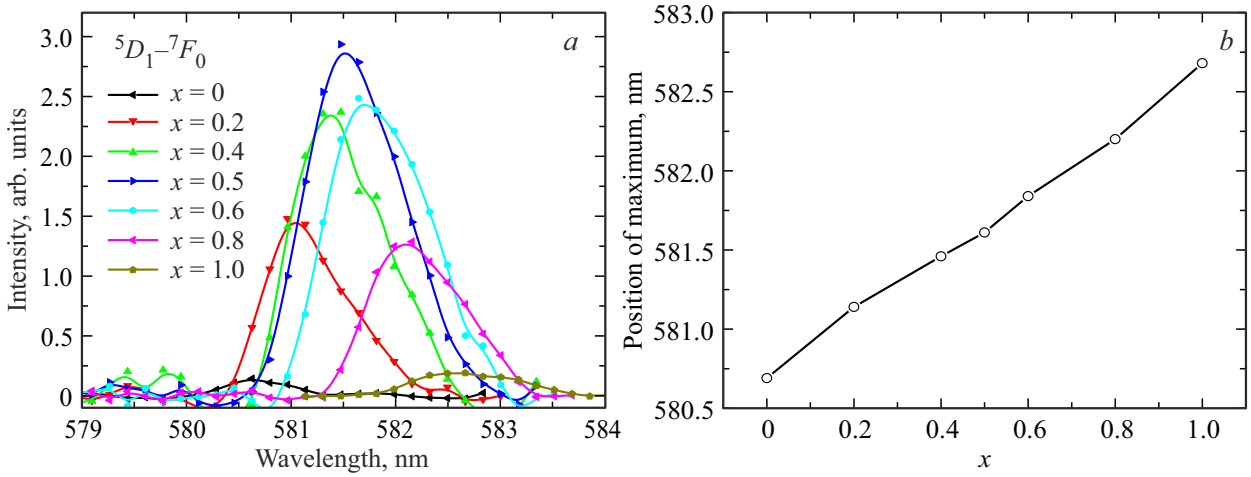

Figure 3. *a* — luminescence spectra of solid solutions $Y_{1-x}Sc_xPO_4:Eu^{3+}$ in the region of $^5D_0(A_1)-^7F_0(A_1)$ transition in Eu^{3+}, $\lambda_{ex} = 397$ nm; *b* — dependence of position of the band maximum on the value of *x*.

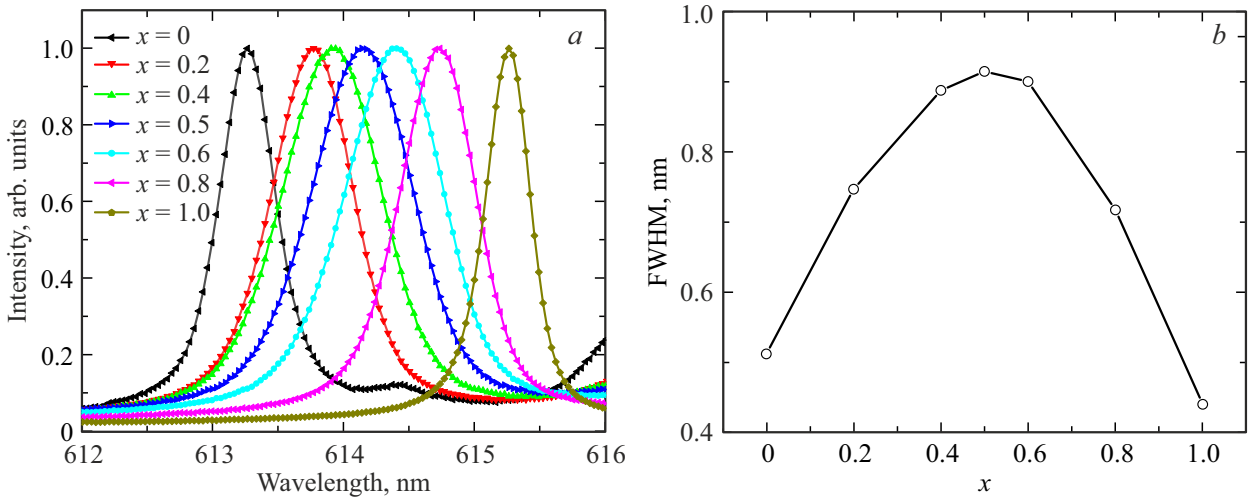

Figure 4. Dependence of position (*a*) and full width at half maximum (*b*) of the band corresponding to the transition $^5D_0(A_1)-^7F_2(B_2)$, $\lambda_{ex} = 397$ nm.

The luminescence spectrum for $ScPO_4:Eu^{3+}$ in the region of $^5D_0-^7F_1$ is represented by only one intensive band at 595.35 nm despite the fact that a doublet at 592.70 and 595.95 nm is observed for the isostructural $YPO_4:Eu^{3+}$. We can assume that this is related to a higher symmetry of the center where Eu^{3+} is located in $ScPO_4$ as compared to YPO_4. This hypothesis is indirectly confirmed by a change of the coefficient of asymmetry in solid solutions under a transition from Y to Sc (Fig. 6). The coefficient of asymmetry is determined as the ratio of integral intensity of the $^5D_0-^7F_2$ transition to $^5D_0-^7F_1$ [26]. When the scandium concentration in the series of solid solutions $Y_{1-x}Sc_xPO_4:Eu^{3+}$ increases, intensity of the $^5D_0-^7F_1$ transition increases as compared to intensity of the $^5D_0-^7F_2$ transition. The highest intensity of the luminescence band, corresponding to the $^5D_0-^7F_1$ transition, was found for the sample of the extreme composition $ScPO_4:Eu^{3+}$. Symmetry of the Eu^{3+} environment in systems, where the $^5D_0-^7F_1$ transition prevails, must be higher because the $^5D_0-^7F_1$ transition is a magnetic dipole one and is permitted by the Laporte rule. Other transitions from the $^5D_0$ level, including $^5D_0-^7F_2$, are electric dipole ones and prohibited by the Laporte rule. The prohibition on them can be partially withdrawn due to a decrease of symmetry of the center where Eu^{3+} is located.

Symmetry of the coordination environment can be also estimated from X-ray data by calculating the coordination polyhedron distortion index (DI):

$$\mathrm{DI} = \frac{1}{n}\sum_{i=1}^{n}\frac{|l_i - l_{av}|}{l_{av}},$$

where n is the coordination number of the central atom, l_i is the distance from the central atom to O atom and

l_{av} is the average distance in the polyhedron. The data about bond lengths were taken from the revised data about the crystal structure of YPO_4 and $ScPO_4$ [21]. A calculation performed on the basis of the literature data shows that DI for the ScO_8 (0.0241) polyhedron is higher as compared to YO_8 (0.0117, Fig. 2). This manifests itself, in particular, in the fact that the ScO_8 polyhedron is more elongated along axis c as compared to YO_8 (Fig. 2). As a result, the oxygen coordination environment of Sc is more distorted as compared to Y, which presuppose a lower point symmetry of the center and contradicts the hypothesis of a higher point symmetry of the luminescence center in scandium phosphate. It should be noted that the given DI calculation does not take into account changes in the environment symmetry upon substitution of yttrium and scandium cations by europium. The ionic radii of Y^{3+} and Eu^{3+} cations are close to (1.02 and 1.087 Å), so we can assume similar coordination environments of these cations. However, the coordination environment of the EuO_8 polyhedra may differ considerably from the one for distorted ScO_8 polyhedra, due to a significant difference of the ionic radii of Sc^{3+} and Eu^{3+} (0.87 and 1.087 Å), which may lead to additional distortions.

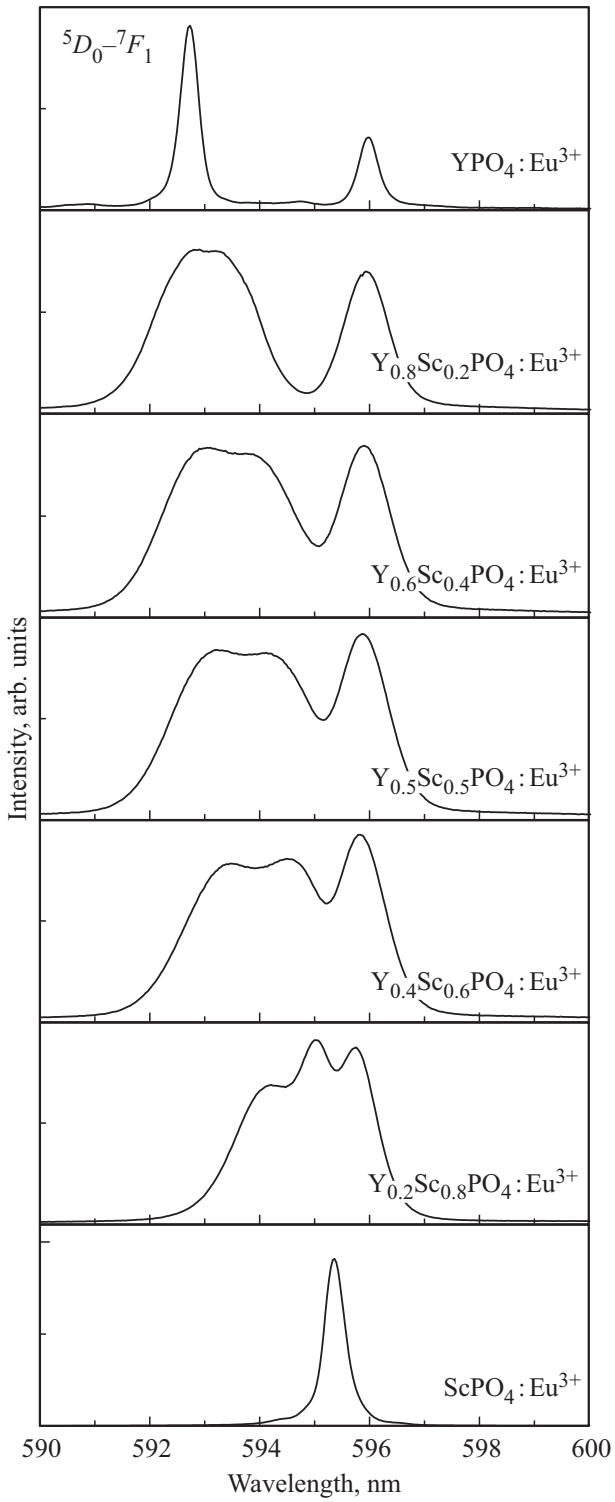

Figure 5. Luminescence spectra of solid solutions $Y_{1-x}Sc_xPO_4:Eu^{3+}$ in the region of transition $^5D_0-^7F_1$, $\lambda_{ex} = 397$ nm.

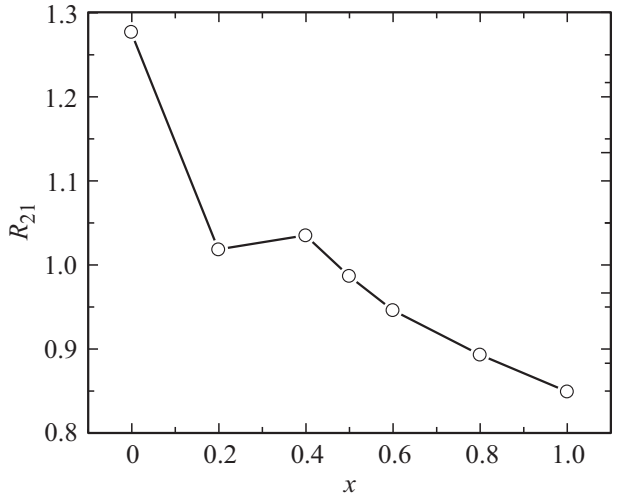

Figure 6. Coefficient of asymmetry (R_{21}) vs. composition of solid solution $Y_{1-x}Sc_xPO_4:Eu^{3+}$.

It should be also noted that one band, corresponding to the $^5D_0-^7F_1$ transition, can be observed only for high-symmetry point groups: T, Th, Td, O, Oh [27]. The maximum quantity of components, corresponding to the $^5D_0-^7F_2$ transition, cannot exceed one, while the experiment results show two pronounced bands at 615.15 and 620.65 nm (Fig. 1). Thus, we can assume than the bands, corresponding to the $^5D_0-^7F_1$ transition in $ScPO_4:Eu^{3+}$, are located sufficiently close to one another and the spectral resolution of the used equipment (0.3 nm) does not allow for resolving them.

3.2. Luminescence excitation spectra $Y_{1-x}Sc_xPO_4:Eu^{3+}$

The luminescence excitation spectra of $Y_{1-x}Sc_xPO_4:Eu^{3+}$ in the region of 2.5–10 eV are shown in Fig. 7. The region of 2.5–4.5 eV, features several

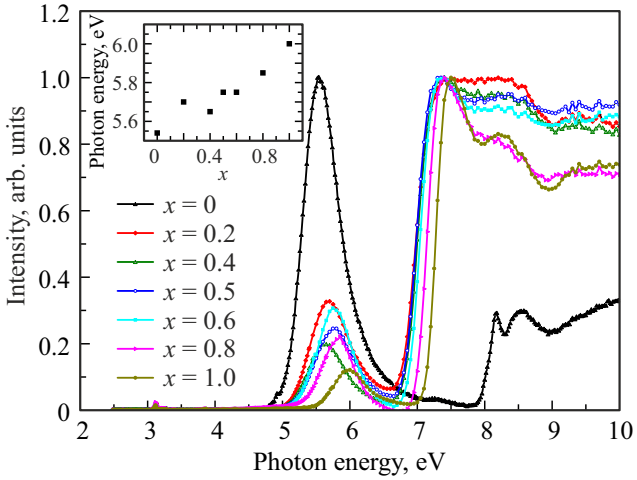

Figure 7. Luminescence excitation spectra of $Y_{1-x}Sc_xPO_4:Eu^{3+}$, $\lambda_{em} = 600$ nm. The inset shows the dependence of position of the maximum for the charge transfer band on the value of x.

narrow low-intensity bands which correspond to intracenter excitation and are typical for intraconfiguration $4f-4f$ transitions in Eu^{3+} [16]. The region of 5–7 eV features an intensive wide excitation band — a charge transfer band. The position of the band maximum shifts by 0.5 eV into the high-energy region when the Sc concentration in $Y_{1-x}Sc_xPO_4:Eu^{3+}$ increases (Fig. 7). The charge transfer band is related to electron transitions from the upper edge of the valence band, formed by $2p$ O, to the ground state $4f^7$ of Eu^{2+} [28]. According to [29], electrons at the $4f^n$ levels are virtually fully shielded from the external crystalline field, that's why the energy position of the levels in Eu does not change significantly for the whole series of the studied solid solutions. Thus, a change of the position of the maximum of the charge transfer band in the series of solid solutions indicates a change of the energy position of the upper edge of the valence band, formed by the $2p-O$ states.

With a further increase of energy $E_{ex} > 6.5$ eV, the luminescence excitation spectra have an abrupt increase of luminescence intensity, which is related to electron transitions in the region of the excitonic absorption band on the fundamental absorption edge. The optical band gap E_g^{opt} can be estimated by interpolating the intensity growth threshold in the excitation spectra to the axis of abscissas (Fig. 8, *a*). The values of E_g^{opt} obtained for YPO_4 (7.93 ± 0.41 eV) and $ScPO_4$ (7.12 ± 0.37 eV) agree with the literature data [23,30,31]. The optical bandgap in solid solutions changes nonlinearly within 7.93 ± 0.41 eV ($x = 0$) to 6.73 ± 0.39 eV ($x = 0.2$) (Fig. 8, *b*). Thereat, the band edge gradually shifts to the low-energy region when x decreases from 1 to 0.2 and abruptly shifts into the region of the higher ones for $x = 0$.

One of the reasons which affects the non-linear pattern of band gap change can be the different nature of the electronic states of the conduction band bottom in the extreme compounds — $ScPO_4$ and YPO_4 [32,33]. A similar effect of a non-linear band gap change (the so-called bowing effect) was observed earlier for solid solutions $Ni_xMg_{1-x}O$, where the $3d$-levels of Ni form a separate subband in the conduction band [34]. The conduction band bottom in $ScPO_4$ is considerably shifted into the low-energy region in relation to YPO_4 and is formed by the $3d$-states of Sc. According to [35], compounds based on Sc^{3+} are characterized by a relatively low energy of the conduction band bottom, which is explained by a strong electronic bond in the scandium $3d$-shell. Thus, local regions on the conduction band bottom arise in solid solution $Y_{1-x}Sc_xPO_4:Eu^{3+}$ already at $x = 0.2$; these regions have an energy close to the position of the conduction band bottom in $ScPO_4$ and determine the obtained value of E_g^{opt}. Indeed, the value of shift of the charge transfer band into the low-energy region (0.38 eV) at a decrease of x

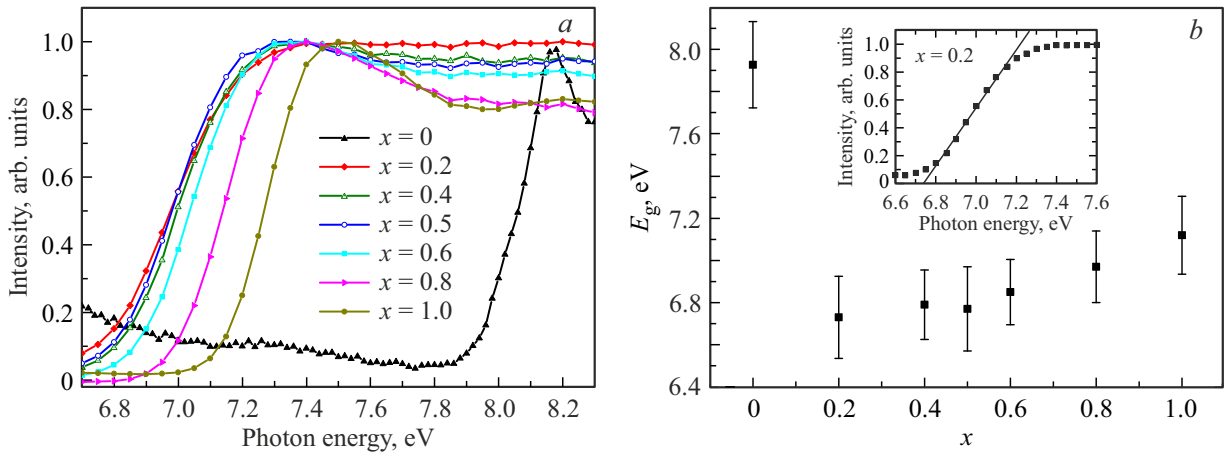

Figure 8. Luminescence excitation spectra of $Y_{1-x}Sc_xPO_4:Eu^{3+}$ in the region of 6.7–8.3 eV (*a*) and dependence of E_g^{opt} on the value of x (*b*). The inset shows: interpolation of the luminescence excitation spectrum in the region of the fundamental absorption edge for $Y_{0.8}Sc_{0.2}PO_4:Eu^{3+}$.

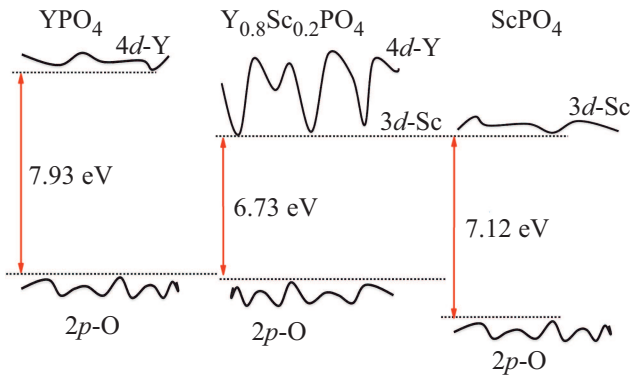

Figure 9. Scheme of change of the conduction band bottom and upper edge of the valence band in $Y_{1-x}Sc_xPO_4$.

from 1 to 0.2 (Fig. 7) corresponds to the value of change of E_g^{opt} (0.39 eV, Fig. 8, *b*). Since the position of the charge transfer band determines the energy position of the upper edge of the valence band, it can be concluded that a band gap change is determined by a shift of the energy position of states of the upper edge of the valence band. It follows from this assumption that the energy position of the electronic states, which form the conduction band bottom, remains constant regardless of scandium concentration in the solution. The scheme of the suggested change of the $Y_{1-x}Sc_xPO_4$ band structure is shown in Fig. 9. The scheme demonstrates that an optical band gap smaller than that of $YPO_4:Eu^{3+}$ and $ScPO_4:Eu^{3+}$ can be obtained for solid solution .$Y_{0.8}Sc_{0.2}PO_4:Eu^{3+}$.

4. Conclusion

A series of solid phosphate solutions $Y_{1-x}Sc_xPO_4$: 0.5 mol.% Eu^{3+} ($x = 0, 0.2, 0.4, 0.5, 0.6, 0.8, 1$) were synthesized by the sol-gel method. A disorder of the crystal structure in solid solutions manifests itself in a change of the structure of Eu^{3+} luminescence spectra, namely — in luminescence band widening and splitting (for degenerate transitions). A disorder also manifests itself in the intensity of the band, which corresponds to the $^5D_0-{}^7F_0$ transition in Eu^{3+} (this transition is prohibited in the D_{2d} point symmetry). The maximum intensity of this transition is observed at $x = 0.5$, which indicates the greatest distortions of symmetry of the luminescence center for the given correlation of substitution cations in the solution. There is also a shift of the said band into the long-wave region when x increases, which is related to a decrease of the Eu–O bond length. In the present paper we have estimated the change of band gap E_g^{opt} depending on solid solution composition. A model of the structure of energy bands in the region of the conduction band bottom and upper edge of the valence band is suggested to explain the nonlinear change of E_g^{opt} with the minimum value of 6.73 ± 0.39 eV at $x = 0.2$.

Funding

The research was funded by the grant of the Russian Science Foundation No. 21-12-00219 (Increasing the efficiency of energy transformation in luminescent and scintillation materials based on solid solutions and composites). D.A. Spassky would like to thank the Estonian Research Council (project PUT PRG111).

Conflict of interest

The authors declare that they have no conflict of interest.

References

[1] W. Di, X. Wang, B. Chen, X. Zhao. Chem. Lett. **34**, *4*, 566 (2005).
[2] V.N. Makhov, N.Yu. Kirikova, M. Kirm, J.C. Krupa, P. Liblik, Ch. Lushchik, E. Negodin, G. Zimmerer. Nucl. Instrum. Meth. Phys. Res. A **486**, *1*, 437 (2002).
[3] R. Mi, Ch. Jian, L. Yan-gai, F. Minghao, M. Lefu, H. Zhaohui, W. Baochen, Z. Chenglong. RSC Adv. **6**, *34*, 28887 (2016).
[4] W. Zheng, H. Zhu, R. Li, D. Tu, Y. Liu, W. Luo, X. Chen. Phys. Chem. Chem. Phys. **14**, *19*, 6974 (2012).
[5] W. Liu, Y. Wang, L. Cheng. J. Am. Ceram. Soc. **94**, *10*, 3449 (2011).
[6] M. Ding, M. Zhang, C. Lu. Mater. Lett. **209**, 52 (2017).
[7] J. Jedoń, J. Zeler, E. Zych. J. Alloys Compd. **816**, 1526603 (2020).
[8] V.S. Levushkina, D.A. Spassky, M.S. Tretyakova, B.I. Zadneprovski, I.A. Kamenskikh, A.N. Vasil'ev, A. Belsky. Opt. Mater. **75**, 607 (2018).
[9] M. Fasoli, A. Vedda, M. Nikl, C. Jiang, B.P. Uberuaga, D.A. Andersson, K.J. McClellan, C.R. Stanek. Phys. Rev. B. **84**, *8*, 081102 (2011).
[10] S.K. Yadav, B.P. Uberuaga, M. Nikl, Ch. Jiang, Ch.R. Stanek. Phys. Rev. Appl. **4**, *5*, 054012 (2015).
[11] A.N. Belsky, E. Auffray, P. Lecoq, C. Dujardin, N. Garnier, H. Canibano, C. Pedrini, A.G. Petrosyan. IEEE Trans. Nucl. Sci. **48**, *4*, 1095 (2001).
[12] O. Sidletskiy, A. Belsky, A.V. Gektin, S. Neicheva, D. Kurtsev, V. Kononets, Christophe Dujardin, K. Lebbou, O. Zelenskaya, V.A. Tarasov, K.N. Belikov, B.V. Grinyov. Cryst. Growth Des. **12**, *9*, 4411 (2012).
[13] D. Spassky, S. Omelkov, H. Mägi, V. Mikhailin, A. Vasil'ev, N. Krutyak, I. Tupitsyna, A. Dubovik, A. Yakubovskaya, A. Belsky. Opt. Mater. **36**, *10*, 1660 (2014).
[14] V.S. Levushkina, V. Mikhailin, D.A. Spassky, B.I. Zadneprovski, M.S. Tretyakova. Phys. Solid State **56**, *11*, 2247 (2014).
[15] A.G. Hernández, D. Boyer, A. Potdevin, G. Chadeyron, A.G. Murillo, F. de J.C. Romo, R. Mahiou. Opt. Mater. **73**, 350 (2017).
[16] D. Spassky, V. Voznyak-Levushkina, A. Arapova, B. Zadneprovski, K. Chernenko, V. Nagirnyi. Symmetry **12**, *6*, 946 (2020).
[17] E.I. Getman, S.V. Radio, L.I. Ardanova. Neorgan. materialy **54**, *6*, 628 (2018).
[18] C. Brecher, H. Samelson, R. Riley, A. Lempicki. J. Chem. Phys. **49**, *7*, 3303 (1968).

[19] W. Dajun, X. Shangda, Y. Min. J. Rare Earths **26**, *3*, 439 (2008).
[20] G. Schimidt, B. Deppisch, V. Gramlich, C. Scheringe. Acta Crystallogr. B **29**, 141 (1973).
[21] W.O. Milligan, D.F. Mullica, G.W. Beall, L.A. Boatner. Inorg. Chim. Acta. **60**, 39 (1982).
[22] R.D. Shannon. Acta crystallogr. A **32**, *5*, 751 (1976).
[23] K. Binnemans. Coordination Chem. Rev. **295**, 1 (2015).
[24] K. Singh, S. Vaidyanathan. Chem. Select **2**, *18*, 5143 (2017).
[25] R.A. Benhamou, A. Bessière, G. Wallez, B. Viana, M. Elaatmani, M. Daoud, A. Zegzouti. J. Solid State Chem. **182**, *8*, 2319 (2009).
[26] I.E. Kolesnikov, A.V. Povolotskiy, D.V. Mamonova, E.Y. Kolesnikov, A.V. Kurochkin, E. Lähderanta, M.D. Mikhailov. J. Rare Earths **36**, *5*, 474 (2018).
[27] P.A. Tanner. Chem. Soc. Rev. **42**, *12*, 5090 (2013).
[28] P. Dorenbos. J. Phys.: Condens. Matter. **15**, *49*, 8417 (2003).
[29] P. Dorenbos. J. Lumin. **91**, *3*, 155 (2000).
[30] A. Trukhin, L.A. Boatner. Materials Science Forum. Trans Tech Publications, Aedermannsdorf, Switzerland **239**, 573 (1997).
[31] L. van Pieterson, M.F. Reid, R.T. Wegh, S. Soverna, A. Meijerink. Phys. Rev. B **65**, *4*, 045114 (2002).
[32] V.S. Levushkina, D.A. Spassky, E.M. Aleksanyan, M.G. Brik, M.S. Tretyakova, B.I. Zadneprovski, A.N. Belsky. J. Lumin. **171**, 33 (2016).
[33] H. Xu, B. Xu, R. Liu, X. Li, S. Zhang, Ch. Ouyang, S. Zhong. Cryst. Eng. Commun. **19**, *38*, 5787 (2017).
[34] C.A. Niedermeier, M. Råsander, S. Rhode, V. Kachkanov, B. Zou, N. Alford, M.A. Moram. Sci. Rep. **6**, 31230 (2016).
[35] P. Dorenbos. J. Phys.: Condens. Matter. **25**, *22*, 225501 (2013).